CSIRO PUBLISHING

International Journal of Wildland Fire **2014**, *23*, 215–223
http://dx.doi.org/10.1071/WF13138

Mapping day-of-burning with coarse-resolution satellite fire-detection data

Sean A. Parks[A,B]

[A]USDA Forest Service, Rocky Mountain Research Station, Aldo Leopold Wilderness Research Institute, 790 East Beckwith Avenue, Missoula, MT 59801, USA. Email: sean_parks@fs.fed.us
[B]Department of Ecosystem and Conservation Sciences, College of Forestry and Conservation, University of Montana, 32 Campus Drive, Missoula, MT 59812, USA.

Abstract. Evaluating the influence of observed daily weather on observed fire-related effects (e.g. smoke production, carbon emissions and burn severity) often involves knowing exactly what day any given area has burned. As such, several studies have used fire progression maps – in which the perimeter of an actively burning fire is mapped at a fairly high temporal resolution – or MODIS satellite data to determine the day-of-burning, thereby allowing an evaluation of the influence of daily weather. However, fire progression maps have many caveats, the most substantial being that they are rarely mapped on a daily basis and may not be available in remote locations. Although MODIS fire detection data provide an alternative due to its global coverage and high temporal resolution, its coarse spatial resolution (1 km^2) often requires that it be downscaled. An objective evaluation of how to best downscale, or interpolate, MODIS fire detection data is necessary. I evaluated 10 spatial interpolation techniques on 21 fires by comparing the day-of-burning as estimated with spatial interpolation of MODIS fire detection data to the day-of-burning that was recorded in fire progression maps. The day-of-burning maps generated with the best performing interpolation technique showed reasonably high quantitative and qualitative agreement with fire progression maps. Consequently, the methods described in this paper provide a viable option for producing day-of-burning data where fire progression maps are of poor quality or unavailable.

Additional keywords: fire progression maps, MODIS, spatial interpolation, weather.

Received 24 August 2013, accepted 25 October 2013, published online 3 February 2014

Introduction

There have been numerous fire-related studies that depended upon knowing the day-of-burning for any given point of any given fire. These studies, for the most part, needed to know the day-of-burning in order to use daily weather (e.g. from a nearby weather station) to explain or predict fire-related phenomena. For example, some studies have evaluated the influence of weather on fire effects (i.e. burn severity) (Collins *et al.* 2007; Bradstock *et al.* 2010; Thompson and Spies 2010) and others have used observed weather data to parameterise their models of fuel consumption and carbon emissions (de Groot *et al.* 2007, 2009). Furthermore, some researchers have parameterised fire simulation models with weather conditions conducive to high spread days (Parisien *et al.* 2011; Parks *et al.* 2011; Podur and Wotton 2011).

The studies described above relied on either fire progression maps or satellite data to infer day-of-burning (and therefore, the ability to determine the associated daily weather). Fire progression maps are often generated by land management and fire agencies, in which the perimeter of an actively burning fire is mapped at a fairly high temporal resolution (every few days to daily). Such fire progression maps are generated using aircraft with GPS or thermal mapping capabilities, aerial photos, ground-based GPS or other field-based intelligence (C. McHugh, pers. comm.). These maps are primarily generated to provide fire managers and the public with information on how a particular wildfire has grown over time. However, they also allow the research community the ability to conduct studies that evaluate, for example, the influence of daily weather on fire effects (e.g. Collins *et al.* 2009; Román-Cuesta *et al.* 2009).

There are some challenges, however, with using day-of-burning data from fire progression maps. First, fire progression maps are rarely created at the resolution of single days because of resource limitation (e.g. no available aircraft during periods of peak fire activity), safety concerns (e.g. high winds or heavy smoke) or remote location (Fig. 1). Generally, only a small number of fires are mapped on a daily basis; these fires tend to be the ones that threaten human life and infrastructure (e.g. 2012 High Park fire in Colorado). More commonly, fire progression maps have temporal gaps, some of them spanning multiple days (Fig. 1). To deal with such gaps, researchers typically average daily weather values over the days where temporal gaps exist in fire progression maps (e.g. Collins *et al.* 2007). Such an approach, however, likely understates the influence of weather because extreme conditions are masked by averaging (Collins *et al.* 2009). Furthermore, because of the limited availability of

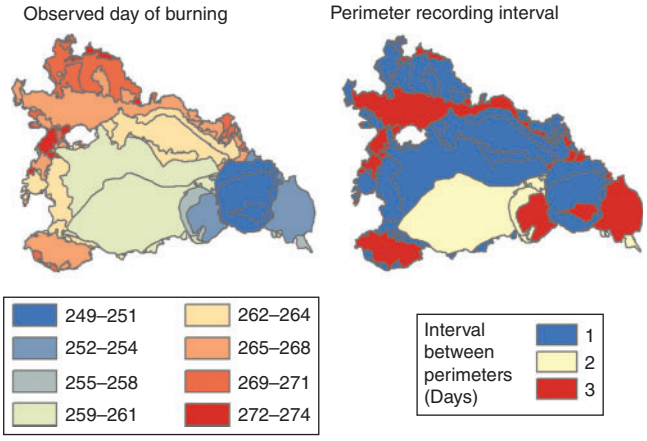

Fig. 1. Julian day the perimeter was recorded (i.e. observed; left) and the number of days that elapsed between perimeter observations (right) for the Day fire in southern California. These maps illustrate that temporal gaps often exist in fire progression maps.

fire progression maps with adequate temporal resolution, many studies have been limited to only one or a few fires, making their findings highly localised. Other caveats of fire progression maps are that collection flight times vary by day, may be attributed with the incorrect day and are sometimes drawn to reflect containment lines and not actual area burned (C. McHugh, pers. comm.; B. Quayle, pers. comm.). Finally, and perhaps most importantly, fire progression maps are often not generated in extremely remote locations (e.g. the Canadian boreal forest).

Where fire progression maps are not available or are of inadequate quality, some researchers have used MODIS fire detection data (NASA MCD14ML product, Collection 5, Version 1) to infer day-of-burning. These satellite data contain the date and location of actively burning pixels but have a coarse spatial resolution (pixel size = 1 km^2). As such, various approaches have been used to downscale them. For example, de Groot *et al.* (2007, 2009) used nearest neighbour interpolation to estimate day-of-burning, whereas Parisien *et al.* (2011) and Parks *et al.* (2012) buffered individual fire detections. Because MODIS fire detection data are collected globally and at a high temporal frequency, they offer an alternative to agency-generated fire progression maps. However, an objective evaluation of how to best interpolate, or downscale, these coarse data is necessary.

There is a clear need by the fire management and research communities for reliable information regarding the day-of-burning for each point within a fire perimeter. Such data would allow a consistent and unbiased method for incorporating daily weather data into fire-related analyses. As such, this study has two objectives: (1) use 10 spatial interpolation techniques to generate fine-scale day-of-burning maps and (2) evaluate each technique using fire progression maps.

Methods

Estimating day-of-burning

I estimated the day-of-burning (DOB) for 21 fires (Table 1) that are greater than 5000 ha and, for comparative purposes, have at least six mapped fire progression perimeters. These fires have broad geographic dispersion (Table 1) to ensure that that the methods evaluated here are applicable across geographic regions. DOB was estimated for each pixel within each fire perimeter using several interpolation techniques (Table 2). Although these estimates can be generated at any resolution, I generated DOB using a pixel size of 30 × 30 m, matching the resolution of Landsat TM imagery and associated products (e.g. burn severity data; Eidenshink *et al.* 2007). All procedures described below are implemented using the R statistical program (R Development Core Team 2007); the code is available from the corresponding author with no restrictions.

Table 1. General information about the 21 study fires, including name, year of burning, size, location (USA state) and duration
Duration is based on first and last MODIS fire detection

Fire name	Year	Size (ha)	Location	Duration (days)
Columbia Cx	2006	53 200	Washington	41
Tripod Cx	2006	74 121	Washington	81
Ahorn	2007	22 699	Montana	57
Corporal	2007	6337	Montana	35
Fool Creek	2007	25 847	Montana	73
Railley Mountain	2007	8576	Montana	48
Showerbath	2007	24 999	Idaho	43
South Barker	2008	13 819	Idaho	53
Twitchell Canyon	2010	18 391	Utah	73
High Park	2012	36 546	Colorado	17
Waldo Canyon	2012	7340	Colorado	8
Rock House	2011	127 640	Texas	22
Miller	2011	36 087	New Mexico	32
Whitewater Baldy	2012	120 508	New Mexico	41
Wallow	2011	221 043	Arizona	28
Day	2006	66 459	S. California	25
Zaca	2007	98 759	S. California	61
Hancock	2006	8964	N. California	81
Pigeon	2006	40 842	N. California	94
Deep	2009	12 242	Florida	6
Mustang Corner	2008	16 166	Florida	6

Estimating DOB was a three step process. In step one, all MODIS fire detection data (NASA MCD14ML product, Collection 5, Version 1) overlapping and within 1 km of the final fire perimeter were selected for use in the interpolation process. Fire perimeters were obtained from the Geospatial Multiagency Coordinating Group (GeoMAC) (2013); non-contiguous polygons (e.g. spot fires) <~100 ha were removed. MODIS fire detection data were obtained from USDA Forest Service Active Fire Mapping Program (http://activefiremaps.fs.fed.us/, accessed 2 December 2013) and serve as the input data for the interpolations. Hereafter, these point data are referred to as MODIS-DOB; they represent MODIS pixel centroids and are attributed with the date that a fire is detected (Fig. 2). MODIS-DOB have a coarse spatial resolution of 1 km^2; however, the high temporal resolution of these data (there are two MODIS sensors, each passing overhead twice per day) provide useful information for mapping fine-scale day-of-burning. In cases where there were two or more spatially coincident fire detections (i.e. fire was detected in the same pixel but on a different day), the one with the earliest date was retained and others were removed.

In step two, I estimated DOB for each pixel within each fire perimeter using 10 interpolation methods (Table 2); hereafter, these DOB estimates are referred to as interpolated-DOB.

Table 2. Abbreviation, name and description of interpolation methods (ordered from simplest to most complex) used to estimate day-of-burning (interpolated-DOB) using coarse resolution MODIS fire detection data (MODIS-DOB)

For those interpolation methods that calculate the average (i.e. AD) or weighted average (i.e. WMD) of nearby MODIS-DOB, I limited the interpolated-DOB to only those dates observed in the nearby MODIS-DOB (See Methods)

Interpolation abbreviation	Interpolation name	Interpolation description
NN	Nearest neighbour	Each pixel is assigned the Julian day of the nearest MODIS fire detection.
ND	Nearest date	Each pixel is assigned the earliest Julian day of the three nearest MODIS fire detections.
AD	Average date	Each pixel is assigned the averaged Julian day of the three nearest MODIS fire detections.
MAJ5	Majority of five nearest neighbours	Each pixel is assigned the most common Julian day among the five nearest fire detections. In case of a tie, the earlier Julian day is assigned.
MAJ10	Majority of 10 nearest neighbours	Each pixel is assigned the most common Julian day among the 10 nearest fire detections. In case of a tie, the earlier Julian day is assigned.
IDW	Inverse distance weighted	Each pixel is assigned a weighted average of the five nearest MODIS fire detections (See Fig. 2). The weight of each fire detection (w_i) is based on the distance (d) and is defined as: $w_i = \left(\frac{1}{d_i}\right) / \sum_{i=1}^{5} 1/d_i$
IDW.sq	Inverse distance weighted-squared	Each pixel is assigned a weighted average of the five nearest MODIS fire detections. The weight of each fire detection (w_i) is based on the distance (d) and is defined as: $w_i = \left(\frac{1}{d_i^2}\right) / \sum_{i=1}^{5} 1/d_i^2$
IDW.half	Inverse distance weighted-square root	Each pixel is assigned a weighted average of the five nearest MODIS fire detections. The weight of each fire detection (w_i) is based on the distance (d) and is defined as: $w_i = \left(\frac{1}{d_i^{0.5}}\right) / \sum_{i=1}^{5} 1/d_i^{0.5}$
WMD	Weighted by mean and distance	Each pixel is assigned a weighted average of the five nearest MODIS fire detections. The weight of each fire detection (w_i) is based on the date ($jday_i$) and distance (d_i) and is defined as: $w_i = \left(\frac{1}{\left(\left\| \left(jday_i - \frac{\left(\sum_{i=1}^{5} jday_i\right)}{5} \right) \right\| + 1 \right) \times d_i} \right)$
WMD.sq	Weighted by mean and distance-squared	Each pixel is assigned a weighted average of the five nearest MODIS fire detections. The weight of each fire detection (w_i) is based on the date ($jday_i$) and distance (d_i) and is defined as: $w_i = \left(\frac{1}{\left(\left\| \left(jday_i - \frac{\left(\sum_{i=1}^{5} jday_i\right)}{5} \right) \right\| + 1 \right)^2 \times d_i} \right)$

The interpolation techniques vary in complexity and not all of them are described in this paragraph; however, the details and equations for all 10 are presented in tabular format (Table 2). The simplest is called nearest neighbour (NN) interpolation, in which each pixel within a fire perimeter is assigned a DOB based on the nearest MODIS-DOB. Moving along the complexity gradient, another is called average date (AD), in which each pixel is assigned a DOB based on the average date of nearby MODIS-DOB data. There are also several interpolation methods that assign DOB to each pixel based on weighted averages of nearby MODIS-DOB data; the most common is inverse-distance weighting (IDW) interpolation (see Fig. 2 for an illustration of how IDW operates). For those interpolation methods that calculate the average (i.e. AD) or weighted average (i.e. WMD) of nearby MODIS-DOB, I limited the interpolated-DOB to only those dates observed in the nearby MODIS-DOB (Table 2). This ensured that the interpolated-DOB corresponded to days of detected fire growth and was not an artefact of averaging. This was accomplished for each pixel by selecting the date of the temporally nearest MODIS-DOB to the average or weighted average of each interpolation method.

In step three, I reassigned all spatially contiguous interpolated-DOB regions that were ≤25 ha to DOB values of the nearest regions larger than 25 ha. This size threshold is admittedly arbitrary; however, this step was necessary because the process described in step two often produced small interpolated-DOB regions that were not in agreement with surrounding estimates. This presumably occurred because of flare ups (and therefore MODIS-DOB detections) that occurred days after the flaming front passed through an area.

Comparison to fire progression maps

To evaluate each interpolation technique, I compared interpolated-DOB to the DOB recorded in fire progression maps obtained from Geospatial Multi-agency Coordinating Group (GeoMAC; 2013); hereafter, GeoMAC-DOB. For any perimeter that was recorded before 1200 hours (noon) on any given day, I changed the recorded DOB to that of the previous day on the assumption that most of the area likely burned the previous afternoon and evening. For example, if a perimeter was recorded at 0400 hours on 2 July, I modified the date of the perimeter and shifted it to 1 July. For this comparison, the GeoMAC-DOB data

are considered the 'observed' data. However, the observed DOB in the GeoMAC-DOB is not necessarily the actual DOB because of temporal gaps in the mapped fire perimeters (Fig. 1); in such cases, I compared the 'recording dates' of the GeoMAC–DOB to aggregated interpolated-DOB. For example, consider a GeoMAC-DOB fire perimeter that was mapped on 1 August and then again on 3 August (i.e. a two-day gap): I used the mapped fire perimeter (GeoMAC-DOB) on 3 August and compared that to the interpolated-DOB for 2 and 3 August. I quantified the percentage of pixels in the interpolated-DOB that *spatially* and *temporally* agreed with the GeoMAC-DOB (i.e. percentage of pixels that exactly matched). I also quantified the percentage of pixels in the interpolated-DOB that were within ±1 and ±2 recording dates of the GeoMAC-DOB. These comparisons, hereafter termed 'percentage agreement', were then used to evaluate each interpolation technique.

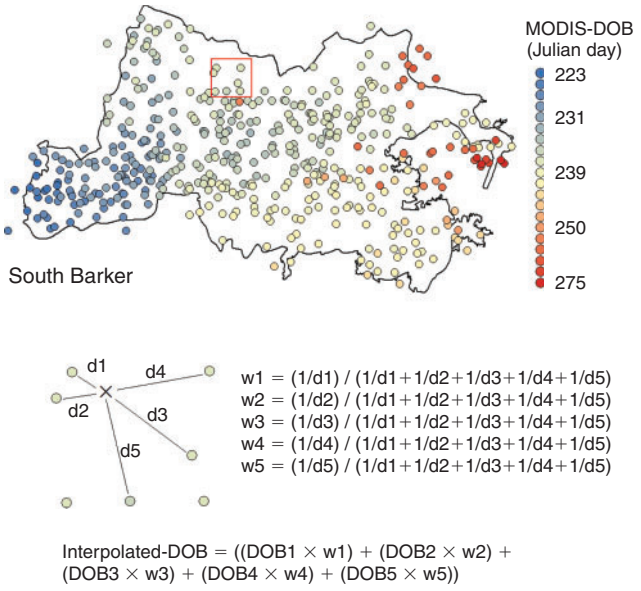

Fig. 2. Illustration of how the inverse distance weighting (IDW) interpolation method operates. For the pixel labelled with an 'X', DOB is estimated using a weighted averaged of the five nearest MODIS fire detections. w1 is the weight (in the IDW weighted average equation (bottom)) of the closest MODIS fire detection, d1 is the distance of the closest fire detection and DOB1 is the day-of-burning of the closest fire detection. w2 is the weight of the second closest MODIS fire detection, etc.

Results

Day-of-burning maps (i.e. interpolated-DOB) for each of the 10 spatial interpolation techniques were generated. Interpolated-DOB, as expected, varied among interpolation techniques, as evaluated qualitatively by the maps (Fig. 3) and quantitatively by the percentage agreement between interpolated-DOB and GeoMAC-DOB (Table 3). Among the 21 fires analysed, the nearest date method (ND) had the lowest mean percentage agreement for the exact match (42.8%), ±1 recording date (69.4%) and ±2 recording dates (80.7%). The weighted by mean and distance method (WMD) had the highest mean percentage agreement for the exact match (46.1%; tied with MAJ10), ±1 recording date (75.8%; tied with WMD.sq) and ±2 recording dates (85.8%; tied with IDW.half and WMD.sq). Taking into account the percentage agreement values for the exact match, ±1 and ±2 recording dates, I conclude that the WMD method performed marginally best overall. However, several other interpolation methods had percentage agreement values that were almost as high as WMD, notably AD, IDW, IDW.sq, IDW.half and WMD.sq. Relative to these top performing methods, the NN, ND, MAJ5 and MAJ10 methods had low percentage agreement with GeoMAC-DOB. Visual inspection of the interpolated-DOB (WMD method) and GeoMAC-DOB also showed good agreement (Fig. 4).

Discussion

Several interpolation methods were effective for mapping DOB for a broad range of ecosystem types, including grass (Mustang Corner, Florida), grass–shrub (Rockhouse, Texas) and conifer-dominated types (Fool Creek, Montana). The average percentage agreement for the WMD method was 46.1% for the exact match, 75.8% for ±1 recording dates and 85.8% for ±2 recording dates. This is approximately in line with the average percentage agreement reported by de Groot *et al.* (2007), who used nearest neighbour interpolation to estimate DOB for one fire in British Columbia, Canada using AVHRR and MODIS fire detections; they found the percentage agreement for ±1 and ±2 recording dates to be 80 and 90% (they did not report the exact match). Although I concluded that the WMD method had the highest percentage agreement when compared with fire progression maps, this was only a marginal improvement over some of the other methods; I therefore suggest that the IDW, IDW.sq, IDW.half and WMD.sq (and to a lesser degree, the AD method) also generate reasonable interpolated-DOB. In fact, these six top-performing interpolation techniques, based on the kappa

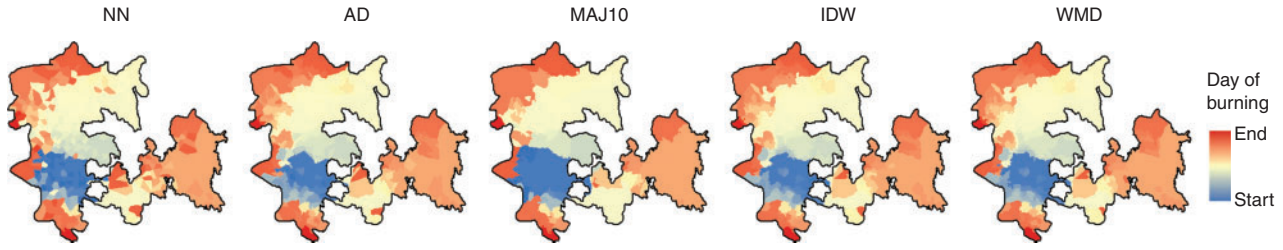

Fig. 3. Visual comparison of five of the interpolation techniques for the Fool Creek fire.

statistic (Landis and Koch 1977), are nearly identical using a kappa = 0.95 threshold (Table 4).

Although MODIS data have coarse spatial resolution, the high temporal resolution of these data supports the use of spatial interpolation techniques and allows DOB maps to be generated at any resolution. This is particularly important, because although fire behaviour and effects are a function of fuels, weather and topography (Agee 1993), the influence of weather is of particular interest (McKenzie *et al.* 2004; Abatzoglou and Kolden 2011) because of its high temporal variability (Bessie and Johnson 1995; Anderson *et al.* 2007) and its dominant influence during extreme years (Moritz 2003; Gedalof *et al.*

Table 3. For each fire, percentage agreement for each interpolation method between the interpolated-DOB and the GeoMAC-DOB for the exact match (±0), within one recording date (±1) and within two recording dates (±2)

NN, nearest neighbor; ND, nearest date; AD, average date; MAJ5, majority of five nearest neighbors; MAJ10, majority of ten nearest neighbors; IDW, inverse distance weighted; IDW.sq, inverse distance weighted – squared; IDW.half, inverse distance weighted – square root; WMD, weighted by mean and distance; WMD.sq, weighted by mean and distance – squared (Table 2)

Fire name	NN			ND			AD			MAJ5			MAJ10		
	±0	±1	±2	±0	±1	±2	±0	±1	±2	±0	±1	±2	±0	±1	±2
Columbia Cx	66.3	84.0	90.4	70.6	86.2	92.2	67.4	86.1	92.0	69.9	85.4	91.1	71.5	86.1	91.5
Tripod Cx	38.7	66.3	77.5	31.5	51.1	59.6	39.2	68.8	79.9	37.3	67.3	78.0	38.5	69.7	80.3
Ahorn	28.5	49.2	63.1	35.0	57.2	70.7	27.2	50.1	67.5	32.4	54.9	70.5	28.4	52.1	69.7
Corporal	31.0	54.2	65.3	35.8	53.4	59.9	32.4	57.5	68.7	33.0	53.8	63.1	34.2	55.0	64.3
Fool Creek	48.1	70.6	79.8	49.1	67.0	77.0	47.9	73.7	80.3	54.9	73.8	81.3	54.5	75.4	83.4
Railley Mountain	45.9	59.4	72.3	77.3	93.9	96.6	44.6	62.3	73.1	43.5	58.7	70.9	43.3	59.9	71.6
Showerbath Cx	36.1	65.9	78.8	45.7	77.7	86.9	38.2	67.8	82.4	31.4	63.1	77.7	31.7	59.4	74.8
South Barker	47.5	78.2	86.5	33.1	60.3	74.1	52.4	84.2	91.4	48.8	82.1	90.3	50.9	82.6	90.9
Twitchell	28.8	51.1	58.3	35.3	59.2	75.6	29.1	54.6	61.1	33.6	54.3	60.0	34.7	54.8	60.0
High Park	51.9	80.6	86.8	49.4	77.3	84.6	54.8	82.6	88.7	54.9	81.2	87.6	56.8	81.9	88.3
Waldo Canyon	59.7	85.1	94.3	54.6	83.5	92.0	63.0	84.8	94.2	64.3	86.5	93.9	64.8	87.7	94.3
Rockhouse	78.4	95.5	97.7	26.2	61.1	75.8	79.4	96.3	97.8	77.9	95.3	97.2	78.7	95.4	97.2
Miller	40.0	69.7	88.3	38.2	63.9	84.7	41.1	72.7	90.4	38.7	68.4	87.7	38.5	66.0	85.9
Whitewater Baldy	41.3	77.6	88.1	43.5	75.8	86.4	42.6	81.3	89.5	42.4	78.7	87.8	41.2	78.8	88.1
Wallow	36.0	75.3	90.1	40.3	78.0	90.7	37.1	77.6	92.2	38.6	77.7	92.2	39.2	76.7	93.1
Day	49.3	83.0	91.8	49.0	83.0	92.1	52.5	85.7	93.1	52.6	85.5	93.0	54.5	86.4	93.4
Zaca	39.2	78.5	87.1	34.0	74.2	86.2	40.5	81.6	90.2	40.9	79.9	88.7	43.0	81.6	89.7
Hancock	50.6	73.3	86.1	42.5	61.9	74.4	51.3	75.3	88.3	46.8	68.0	80.5	50.6	71.4	84.2
Pigeon	38.3	63.5	78.3	41.5	55.6	70.3	40.0	67.2	82.1	37.8	60.3	75.8	39.2	61.4	77.0
Deep	28.4	68.6	84.4	9.9	48.1	72.2	23.6	69.0	85.0	19.6	61.5	79.9	15.4	58.5	75.5
Mustang Corner	60.3	91.9	96.3	55.6	88.5	93.6	57.8	93.7	97.2	58.8	92.6	94.2	58.7	90.8	92.5
MEAN	45.0	72.5	82.9	42.8	69.4	80.7	45.8	74.9	85.0	45.6	72.8	82.9	46.1	72.9	83.1

Fire name	IDW			IDW.sq			IDW.half			WMD			WMD.sq		
	±0	±1	±2	±0	±1	±2	±0	±1	±2	±0	±1	±2	±0	±1	±2
Columbia Cx	66.9	86.5	92.5	66.9	85.9	92.0	66.3	86.8	92.7	67.5	86.7	92.7	67.4	86.9	92.7
Tripod Cx	39.6	69.2	80.6	39.5	69.0	80.1	39.4	69.1	80.8	39.7	69.7	80.9	39.8	69.6	80.9
Ahorn	26.3	49.0	66.4	28.0	49.9	66.6	26.2	49.4	66.3	26.0	49.3	66.7	25.5	48.8	66.5
Corporal	32.4	59.7	70.5	31.9	58.5	69.3	32.5	60.0	70.6	32.3	60.6	71.1	31.8	60.8	71.1
Fool Creek	46.4	73.9	80.3	46.4	73.6	80.1	45.7	74.0	80.5	46.6	74.1	80.7	46.6	74.1	80.8
Railley Mountain	44.8	62.6	74.0	45.2	62.0	73.8	43.5	62.0	73.4	44.0	62.3	73.5	43.9	62.2	73.3
Showerbath Cx	39.9	69.1	84.4	39.5	68.5	83.2	39.6	68.8	84.9	39.7	68.5	84.3	39.6	68.3	84.5
South Barker	52.4	85.3	92.1	51.3	84.6	91.5	52.4	85.4	92.5	52.6	85.1	92.7	53.1	85.5	92.9
Twitchell	29.1	56.7	62.4	28.8	56.0	61.9	29.2	57.2	63.0	29.5	56.7	62.4	29.7	56.8	62.8
High Park	55.0	83.1	89.5	54.8	82.7	88.7	54.4	83.1	89.5	55.0	83.5	89.7	54.8	83.4	89.7
Waldo Canyon	64.2	86.8	95.2	62.3	86.9	95.1	65.5	86.9	95.0	66.0	87.3	95.6	66.2	87.2	95.3
Rockhouse	79.6	96.3	97.8	79.1	96.2	97.8	79.6	96.3	97.7	79.5	96.3	97.7	79.5	96.3	97.7
Miller	41.4	73.6	91.8	41.5	73.3	91.1	41.2	73.0	91.4	41.4	73.5	91.7	41.3	73.2	91.5
Whitewater Baldy	42.9	82.3	90.2	43.3	82.0	90.1	42.4	82.0	90.2	42.7	82.3	90.1	42.7	82.2	90.1
Wallow	37.5	78.3	93.3	37.4	78.0	92.7	37.3	78.0	93.4	37.8	78.6	93.7	37.6	78.3	93.6
Day	53.0	85.9	93.3	52.4	85.6	93.1	53.4	86.0	93.4	53.8	86.2	93.4	54.0	86.2	93.4
Zaca	40.6	82.0	90.4	40.7	81.4	89.9	40.6	81.9	90.4	41.3	82.5	90.6	41.0	82.5	90.6
Hancock	53.7	76.6	89.0	54.8	75.9	89.2	53.4	76.1	89.2	54.6	76.6	88.8	53.7	76.0	89.2
Pigeon	39.4	67.9	83.5	40.0	67.4	83.2	39.3	67.8	83.6	39.5	67.9	83.9	39.5	67.8	83.7
Deep	20.3	69.6	85.7	22.8	69.3	85.5	19.9	69.5	85.5	20.3	69.5	85.5	20.2	69.9	85.5
Mustang Corner	58.4	93.8	97.3	59.2	93.7	97.1	57.3	94.3	97.2	58.0	94.8	97.0	57.8	95.5	97.0
MEAN	45.9	75.6	85.7	46.0	75.3	85.3	45.7	75.6	85.8	46.1	75.8	85.8	46.0	75.8	85.8

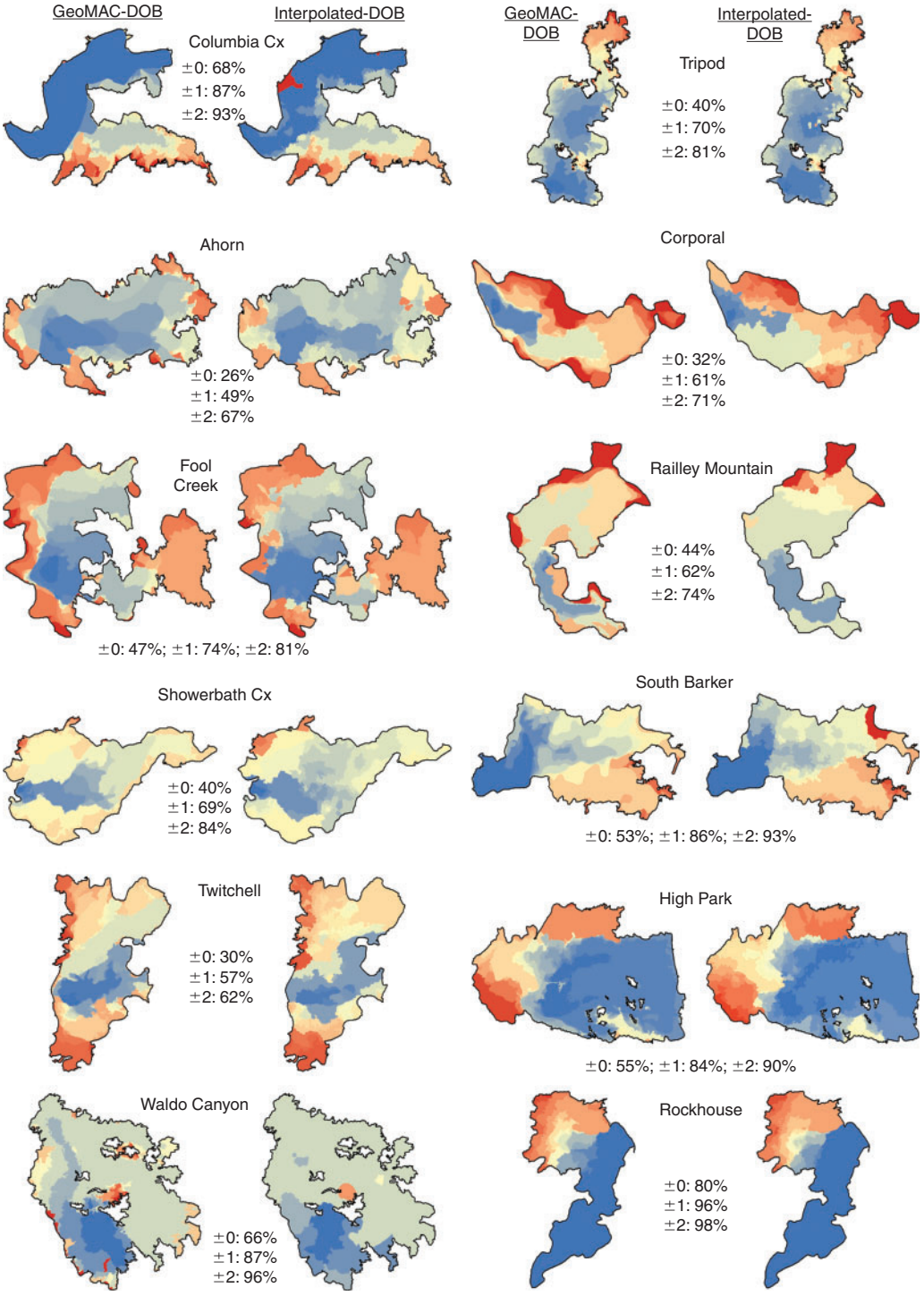

Fig. 4. Maps showing GeoMAC-DOB *v.* interpolated-DOB (WMD) for each of the 21 study fires.

2005). As such, the methodology developed here will allow for incorporating weather data into fire-related analyses covering broad regions and literally hundreds or thousands of fires (e.g. Parks *et al.* 2013). For example, studies that tie weather to wildfire smoke and carbon emissions (McKenzie *et al.* 2006; Lavoué *et al.* 2007) would benefit tremendously from the methods described here. Studies analysing the effect of weather on fire effects (i.e. burn severity) (e.g. Thompson and Spies 2010) would also benefit, as would fire simulation studies that parameterise their models with weather conditions conducive to high spread days (e.g. Parisien *et al.* 2011). A related benefit of using the methods described here is simply the ability to

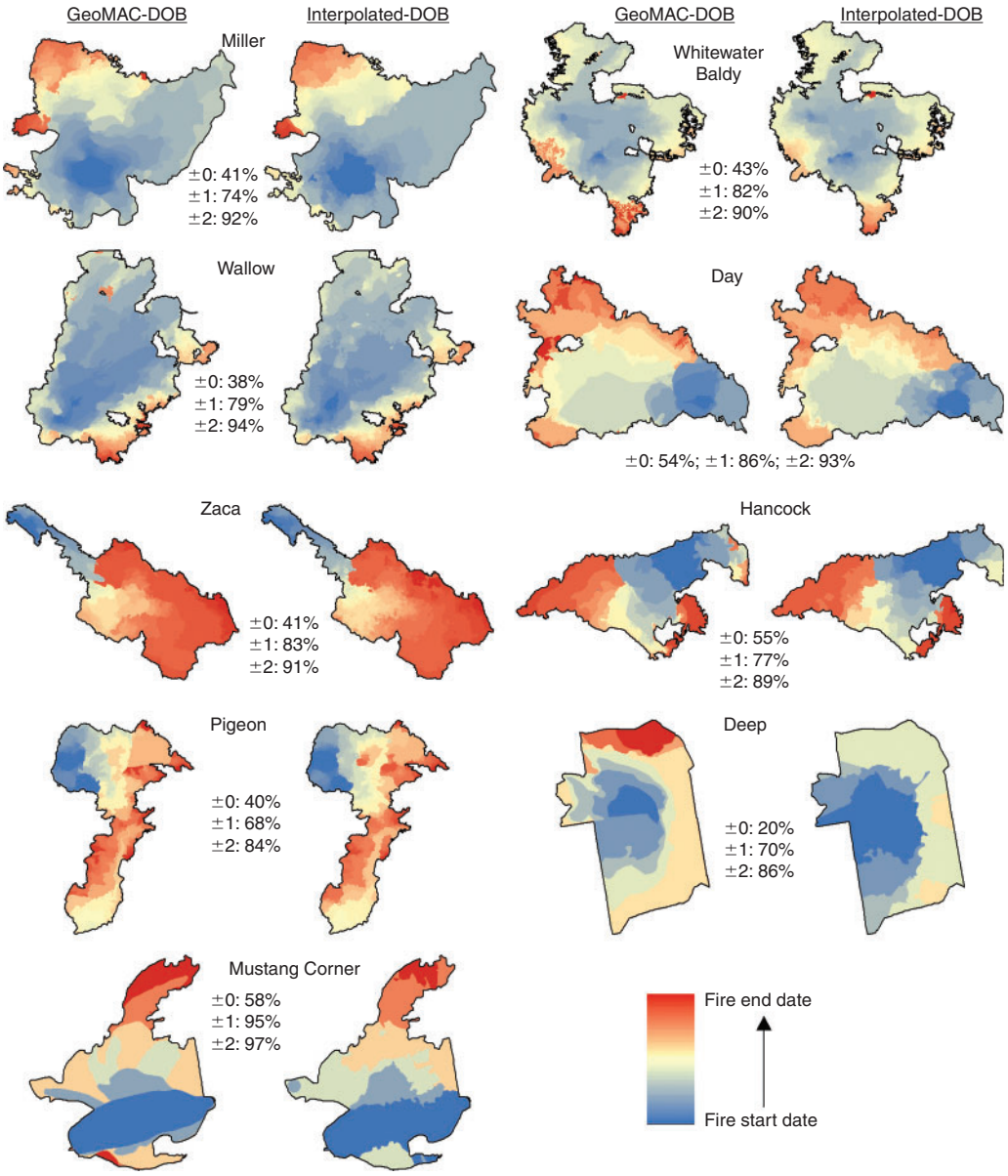

Fig. 4. (Continued)

quantify daily fire growth of individual fires. For example, such an ability would benefit studies like those of Lavoué and Stocks (2011) who used a sigmoidal growth function, based on fire duration and final size, to estimate daily fire growth.

Although I used fire progression maps for quasi-validation purposes, it should be noted that these data are imperfect, as previously described, and are not likely correct themselves. The lack of adequate ground-truthed data is challenging and, as such, complicates the validation procedure: it is not possible to know with 100% confidence how well the interpolations in this study perform. For example, the WMD method, on average, 'under-predicted' the DOB by 0.2 recording dates (average difference between interpolated- and observed-DOB among the 21 fires; range: −1.3 – 0.4); that is, the interpolated-DOB was generally earlier than the recorded-DOB in the fire progression maps. In some cases, this under-prediction was substantial (four fires were <-0.5 recording dates and two fires were <-1.0). Such bias in the interpolations are likely due to incorrect recording dates of the fire progression maps, as it is highly unlikely that the MODIS satellite would systematically detect a fire before it actually burned. Considering the previously described caveats with fire progression maps and that they may, on average, systematically record the fire date later than it occurred, it is possible that the percentage agreement values reported in this study underestimate the quality of the interpolations.

The methodology developed in this paper has been shown to generate, on average, robust DOB estimates. However, there are some reasons why estimated DOB may be incorrect in some areas. Clouds, heavy smoke and tree canopy may limit the ability

Table 4. Average (among all 21 fires) kappa statistic (Landis and Koch 1977) between all pairwise interpolation techniques

NN, nearest neighbor; ND, nearest date; AD, average date; MAJ5, majority of five nearest neighbors; MAJ10, majority of ten nearest neighbors; IDW, inverse distance weighted; IDW.sq, inverse distance weighted – squared; IDW.half, inverse distance weighted – square root; WMD, weighted by mean and distance; WMD.sq, weighted by mean and distance – squared (Table 2)

	NN	ND	AD	MAJ5	MAJ10	IDW	IDW.sq	IDW.half	WMD	WMD.sq
NN	–	–	–	–	–	–	–	–	–	–
ND	0.84	–	–	–	–	–	–	–	–	–
AD	0.92	0.88	–	–	–	–	–	–	–	–
MAJ5	0.87	0.90	0.92	–	–	–	–	–	–	–
MAJ10	0.85	0.88	0.89	0.91	–	–	–	–	–	–
IDW	0.92	0.87	0.96	0.92	0.90	–	–	–	–	–
IDW.sq	0.94	0.87	0.96	0.91	0.89	0.98	–	–	–	–
IDW.half	0.91	0.88	0.96	0.93	0.90	0.99	0.97	–	–	–
WMD	0.91	0.88	0.96	0.93	0.90	0.99	0.97	0.99	–	–
WMD.sq	0.91	0.88	0.96	0.93	0.90	0.98	0.96	0.99	0.99	–

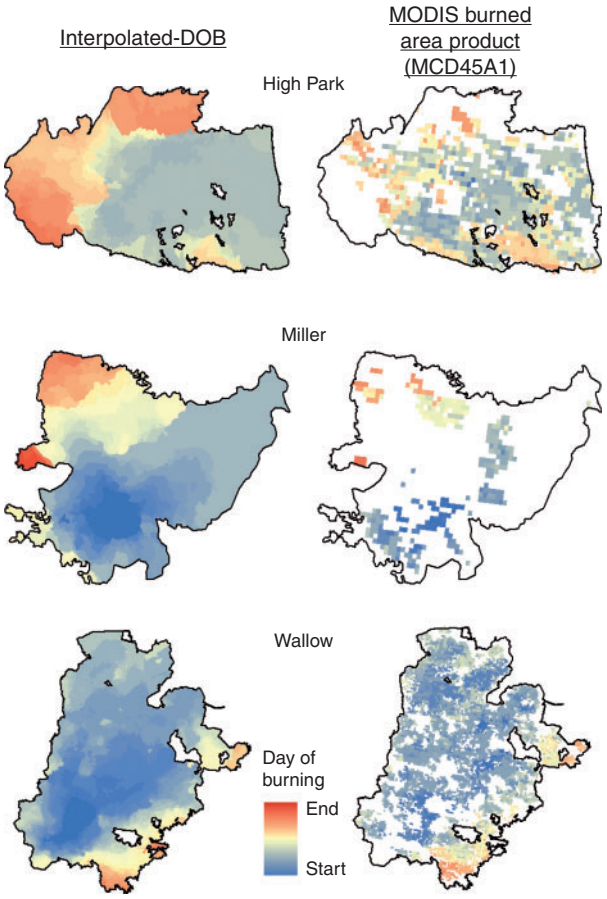

Fig. 5. Interpolated (left) and MODIS burned area product (MCD45A1; right) day-of-burning for High Park, Miller and Wallow fires.

of the MODIS sensors from detecting fire (Giglio 2010). Also, individual pixels within fast moving or low intensity fires may not be detected. Additional mischaracterisation of DOB is likely due to the coarse resolution of the fire detection data. Also because of the coarse resolution of the MODIS data, it is likely that the methods described here are inappropriate for small fires (<~500 ha); note that the smallest fire I analysed was ~6300 ha. There are other inherent caveats associated with the fire detection algorithm (e.g. varying levels of detection confidence) (Giglio 2010) and remote sensing in general (Verstraete *et al.* 1996). Finally, it may be that the methods developed here are not necessary when high-quality daily fire progression maps are available. Although these caveats are important considerations, the methods described in this paper provide a viable option for producing DOB data where agency-generated fire progression maps are of poor quality or unavailable.

Finally, it is worth noting that the MODIS burned area product (MCD45A1) (Roy *et al.* 2005) also estimates DOB by evaluating change in vegetation. However, it has an eight-day precision (Roy and Boschetti 2009) and oftentimes has spatial gaps within a fire perimeter (i.e. no data on estimated DOB for some MODIS pixels) (Fig. 5). As such, the methods presented in this paper can potentially be used to complement other algorithms that estimate DOB (e.g. Giglio *et al.* 2009).

Acknowledgements

I thank A. Scalise for GIS assistance and S. Dobrowski, R. Keane, A. Larson, C. Miller, M-A. Parisien, B. Quale and C. Nelson for thoughtful comments that significantly improved this manuscript. I acknowledge National Fire Plan funding from the USDA Forest Service, Rocky Mountain Research Station.

References

Abatzoglou JT, Kolden CA (2011) Relative importance of weather and climate on wildfire growth in interior Alaska. *International Journal of Wildland Fire* **20**, 479–486. doi:10.1071/WF10046

Agee JK (1993). 'Fire Ecology of Pacific Northwest Forests.' (Island Press: Washington, DC.)

Anderson K, Reuter G, Flannigan MD (2007) Fire-growth modelling using meteorological data with random and systematic perturbations. *International Journal of Wildland Fire* **16**, 174–182. doi:10.1071/WF06069

Bessie WC, Johnson EA (1995) The relative importance of fuels and weather on fire behavior in subalpine forests. *Ecology* **76**, 747–762. doi:10.2307/1939341

Bradstock RA, Hammill KA, Collins L, Price O (2010) Effects of weather, fuel and terrain on fire severity in topographically diverse landscapes of

south-eastern Australia. *Landscape Ecology* **25**, 607–619. doi:10.1007/S10980-009-9443-8

Collins BM, Kelly M, van Wagtendonk JW, Stephens SL (2007) Spatial patterns of large natural fires in Sierra Nevada wilderness areas. *Landscape Ecology* **22**, 545–557. doi:10.1007/S10980-006-9047-5

Collins BM, Miller JD, Thode AE, Kelly M, van Wagtendonk JW, Stephens SL (2009) Interactions among wildland fires in a long-established Sierra Nevada natural fire area. *Ecosystems* **12**, 114–128. doi:10.1007/S10021-008-9211-7

de Groot WJ, Landry R, Kurz WA, Anderson KR, Englefield P, Fraser RH, Hall RJ, Banfield E, Raymond DA, Decker V, Lynham TJ, Pritchard JM (2007) Estimating direct carbon emissions from Canadian wildland fires. *International Journal of Wildland Fire* **16**, 593–606. doi:10.1071/WF06150

de Groot WJ, Pritchard JM, Lynham TJ (2009) Forest floor fuel consumption and carbon emissions in Canadian boreal forest fires. *Canadian Journal of Forest Research* **39**, 367–382. doi:10.1139/X08-192

Eidenshink J, Schwind B, Brewer K, Zhu ZL, Quayle B, Howard S (2007) A project for monitoring trends in burn severity. *Fire Ecology* **3**, 3–21. doi:10.4996/FIREECOLOGY.0301003

Gedalof Z, Peterson DL, Mantua NJ (2005) Atmospheric, climatic, and ecological controls on extreme wildfire years in the northwestern United States. *Ecological Applications* **15**, 154–174. doi:10.1890/03-5116

Geospatial Multi-agency Coordinating Group (GeoMAC) (2013). Fire perimeter dataset. Available at http://rmgsc.cr.usgs.gov/outgoing/GeoMAC [Verified 2 December 2013]

Giglio L (2010). MODIS collection 5 active fire product user's guide. (University of Maryland, Department of Geography) Available at http://www.fao.org/fileadmin/templates/gfims/docs/MODIS_Fire_Users_Guide_2.4.pdf [Verified 2 December 2013]

Giglio L, Loboda T, Roy DP, Quayle B, Justice CO (2009) An active-fire based burned area mapping algorithm for the MODIS sensor. *Remote Sensing of Environment* **113**, 408–420. doi:10.1016/J.RSE.2008.10.006

Landis JR, Koch GG (1977) Application of hierarchical Kappa-type statistics in assessment of majority agreement among multiple observers. *Biometrics* **33**, 363–374. doi:10.2307/2529786

Lavoué D, Stocks BJ (2011) Emissions of air pollutants by Canadian wildfires from 2000 to 2004. *International Journal of Wildland Fire* **20**, 17–34. doi:10.1071/WF08114

Lavoué D, Gong S, Stocks BJ (2007) Modelling emissions from Canadian wildfires: a case study of the 2002 Quebec fires. *International Journal of Wildland Fire* **16**, 649–663. doi:10.1071/WF06091

McKenzie D, Gedalof ZE, Peterson DL, Mote P (2004) Climatic change, wildfire, and conservation. *Conservation Biology* **18**, 890–902. doi:10.1111/J.1523-1739.2004.00492.X

McKenzie D, O'Neill SM, Larkin NK, Norheim RA (2006) Integrating models to predict regional haze from wildland fire. *Ecological Modelling* **199**, 278–288. doi:10.1016/J.ECOLMODEL.2006.05.029

Moritz MA (2003) Spatiotemporal analysis of controls on shrubland fire regimes: Age dependency and fire hazard. *Ecology* **84**, 351–361. doi:10.1890/0012-9658(2003)084[0351:SAOCOS]2.0.CO;2

Parisien MA, Parks SA, Miller C, Krawchuk MA, Heathcott M, Moritz MA (2011) Contributions of Ignitions, Fuels, and weather to the burn probability of a boreal landscape. *Ecosystems* **14**, 1141–1155. doi:10.1007/S10021-011-9474-2

Parks SA, Parisien MA, Miller C (2011) Multi-scale evaluation of the environmental controls on burn probability in a southern Sierra Nevada landscape. *International Journal of Wildland Fire* **20**, 815–828. doi:10.1071/WF10051

Parks SA, Parisien M-A, Miller C (2012) Spatial bottom-up controls on fire likelihood vary across western North America. *Ecosphere* **3**, art12. doi:10.1890/ES11-00298.1

Parks SA, Miller C, Nelson CR, Holden ZA (2013) Previous fires moderate burn severity of subsequent wildland fires in two large western US wilderness areas. *Ecosystems.* [Published online early 10 September 2013]

Podur J, Wotton BM (2011) Defining fire spread event days for fire-growth modelling. *International Journal of Wildland Fire* **20**, 497–507. doi:10.1071/WF09001

R Development Core Team (2007). 'R: a language and environment for statistical computing.' (R Foundation for Statistical Computing: Vienna, Austria)

Román-Cuesta RM, Gracia M, Retana J (2009) Factors influencing the formation of unburned forest islands within the perimeter of a large forest fire. *Forest Ecology and Management* **258**, 71–80. doi:10.1016/J.FORECO.2009.03.041

Roy DP, Boschetti L (2009) Southern Africa validation of the MODIS, L3JRC, and GlobCarbon burned-area products. *IEEE Transactions on Geoscience and Remote Sensing* **47**, 1032–1044. doi:10.1109/TGRS.2008.2009000

Roy DP, Jin Y, Lewis PE, Justice CO (2005) Prototyping a global algorithm for systematic fire-affected area mapping using MODIS time series data. *Remote Sensing of Environment* **97**, 137–162. doi:10.1016/J.RSE.2005.04.007

Thompson JR, Spies TA (2010) Factors associated with crown damage following recurring mixed-severity wildfires and post-fire management in southwestern Oregon. *Landscape Ecology* **25**, 775–789. doi:10.1007/S10980-010-9456-3

Verstraete MM, Pinty B, Myneni RB (1996) Potential and limitations of information extraction on the terrestrial biosphere from satellite remote sensing. *Remote Sensing of Environment* **58**, 201–214. doi:10.1016/S0034-4257(96)00069-7